11.2 GEOGRAPHICAL AND SEASONAL AVAILABILITY OF LIGHT RAIN, DRY SNOW, AND BRAGG SCATTER TO ESTIMATE WSR-88D Z_{DR} SYSTEM BIAS

W. David Zittel*, Robert R. Lee, Lindsey M. Richardson, Jeffrey G. Cunningham, Jessica A. Schultz, and Richard L. Ice

Radar Operations Center
1200 Westheimer Drive
Norman, Oklahoma

1. INTRODUCTION

In 2013 the United States government completed an upgrade of its 160 operational Weather Surveillance Radars – 1988D (WSR-88Ds) to dual polarization. One of the main objectives of this upgrade was to provide improved Quantitative Precipitation Estimates (QPE) using information obtained from differential reflectivity (Z_{DR}). Z_{DR}, or the ratio of the received horizontal power and the vertical power, provides measures of the oblateness of rain drops, which along with the return power from the horizontal channel, can be used empirically to derive rainfall rates for light, moderate, and heavy rain. The equation, from Bringi and Chandrasekar (2001), has the form:

$$R(Z, Z_{DR}) = 6.7010^{-3} Z^{0.927} Z_{DR}^{-3.43} \quad (1)$$

where R is rainrate in mm hr^{-1}, Z is reflectivity in dBZ, and Z_{DR} is the differential reflectivity in dB. It can be shown that a 0.25 dB increase in the Z_{DR} bias yields a decrease in rainrate of ~22% and thus in rainfall accumulation.

The WSR-88D currently uses four methods to estimate Z_{DR} bias: 1) an engineering derived method; 2) a light rain method; 3) a dry snow method; and 4) a Bragg scattering method. The goal is to make the Z_{DR} estimate as accurate as possible to provide the best rainfall accumulation estimates. This paper discusses findings from the first full year of analyses of the three meteorological Z_{DR} bias estimators.

*Corresponding Author: W. David Zittel, Radar Operations Center, 1200 Westheimer Drive, Norman, Oklahoma 73069
email: walter.d.zittel@noaa.gov

2. BACKGROUND

Previous research has determined that an accuracy in the measured Z_{DR} bias of ± 0.1 dB is desirable and achievable (Ryzhkov et al. 2005). For acceptance testing, the contractor had merely to demonstrate via a desktop exercise that measured path losses in the receiver, transmitter, and antenna bias yielded the desired accuracy. In practice, this "engineering-derived" method has proven challenging to achieve and verify independently (Ice et al. 2013; Ice et al. 2014). An estimate of the bias (updated each volume scan) is applied to the measured Z_{DR} that is sent in the data stream from the WSR-88D's Radar Data Acquisition (RDA) Unit to its Radar Product Generator (RPG) Unit. This data stream is called Level II data. Also provided in the data stream is the estimated bias itself and is labeled ZDRB. In parallel with engineering methods under development (such as cross-polarization measurements) to independently verify system Z_{DR} bias, the ROC Applications Branch has developed techniques to examine external meteorological targets under conditions where the intrinsic Z_{DR} bias is either 0 dB or can be corrected to near 0 dB.

3. METHODS FOR ESTIMATING SYSTEM Z_{DR} BIAS FROM RADAR ECHO

The ROC currently uses three types of meteorological returns to estimate system Z_{DR} bias. They are light rain, dry snow, and Bragg scatter. These techniques have been described in detail (Cunningham 2013; Zittel 2014). Figure 1 shows schematically that light rain is sampled below the melting layer while dry snow, which ideally is dry "aggregate" snow, is sampled above the melting layer. Figure 2 shows schematically the source of Bragg scatter from turbulent eddies often found at the top of the convective boundary

layer during midday heating. However, strongly sheared winds with minimal moisture and temperature discontinuities may also provide Bragg scatter (Ottersten 1969). Ideally, returns come from either a different regime within a precipitation event or when there is no precipitation. (See Figures 1 and 2.)

By estimating Z_{DR} bias from light rain and dry snow in precipitation and Bragg scattering in clear air, we optimize opportunities to acquire estimates of system Z_{DR} bias. These three methods work with operational scanning strategies and do not impact live operations.

For the precipitation events, identification of the melting layer is critical to the success of the light rain and dry snow events. Giangrande et al. (2008) provides a description of the WSR-88D's Melting Layer Algorithm. Under subfreezing conditions no melting layer is present. Clouds and light snow may have characteristics similar to Bragg scatter so proper filtering here is key to providing good estimates.

3.1 Light Rain

Gorgucci (1999) proposed that system Z_{DR} bias could be determined by pointing a radar at the zenith (90°). Rotating the radar through 360° and averaging Z_{DR} during light rain events should eliminate biases contributed by ground clutter and non-zero canting angles of rain drops. The mean Z_{DR} thus obtained should reflect the system Z_{DR} bias due to unequal paths or gains in the horizontally and vertically polarized channels. Frech (2013) describes real-time implementation of this technique by the Deutscher Wetterdienst.

The WSR-88D inherently cannot be pointed vertically due to mechanical constraints. Instead, reflectivity data bins between 19 and 30.5 dBZ are tabulated in 2 dBZ increments and averages of Z_{DR} associated with the reflectivity data are computed. The reflectivity data must be above 1° in elevation, at a minimum distance of 20 km from the radar and at least 1 km below the lower half-power point of where the radar beam intercepts the melting layer. Empirical adjustments to the average Z_{DR} for each reflectivity interval (Table 1) are based on disdrometer measurements made in Oklahoma (Schuur et al. 2001; Schuur et al. 2005).

Table 1. For each of 6 reflectivity categories this table shows empirical offsets subtracted from estimates of system Z_{DR} bias derived from light rain.

19.0 - 20.5 dBZ	21.0 - 22.5 dBZ	23.0 - 24.5 dBZ	25.0 - 26.5 dBZ	27.0 - 28.5 dBZ	29.0 - 30.5 dBZ
0.23 dB	0.27 dB	0.32 dB	0.38 dB	0.46 dB	0.55 dB

An average of the Z_{DR} found for each of the 6 categories in Table 1 is computed for each volume scan. Even with such averaging, estimates of Z_{DR} bias show great variability from one volume scan to another. The Z_{DR} bias estimates for each reflectivity interval are saved in a log file and archived at the National Climatic Data Center (NCDC) every 8 hours. MATLAB code retrieves the log files for further processing.

To reduce the volume-to-volume variability, a minimum of 3 hours of continuous data must be collected. The period may be expanded to 6 hours if there is no more than a 1-hour break in the availability of Z_{DR} bias estimates. A median value over the 3-hour period is computed. A maximum of 4 estimates per day are generated. The median value of all available light rain estimates during a month provides an estimate of the monthly Z_{DR} bias.

3.2 Dry Snow

The estimation of a system Z_{DR} bias based on dry snow assumes that the dry snow consists of small aggregates that are spherical and tumbling, and, therefore, would have no preferred orientation with respect to either the horizontal or vertical channels. That is, the bias for Z_{DR} should be ~0 dB. Straka et al. (2000), in a survey of literature on expected ranges of values for dual polarization parameters, suggests a range of 0.0 to 0.5 dB for Z_{DR} in dry aggregate snow for C band radars. Thompson et al. (2014), in developing a winter hydrometeor classification algorithm, used Z_{DR} values for aggregates of near 0 dB for X, C, and S band radars. The authors have found that a downward adjustment of 0.2 dB for Z_{DR} estimates of dry snow yields results similar to the light rain and Bragg scatter methods.

To minimize possible contamination from ice crystals, data within the kilometer immediately above the melting layer is examined. The upper boundary of the melting layer is the height at which the lower half-power beam exits the melting layer. As with the light rain, averages of Z_{DR} are computed for all bins satisfying the height requirements.

This method uses regions identified as dry snow by the Hydrometeor Classification Algorithm (HCA) algorithm (Straka 2000; Hyang Suk et al. 2009). To minimize contamination from ground clutter the method obtains data at all elevation angles greater than 1° that meet the height requirement with reflectivity volume sample values between 15 and 25 dBZ. Three filters are applied to the dry snow radar bins: signal-to-noise ratio (SNR) ≥ 20 dB; $0.98 < RHO_{HV} < 1.0$ to ensure sure strong signal is

processed in the uniform dry snow region; and PHI_{DP} < 100° to ensure the beam is not sampling heavy precipitation. For each volume scan there must be at least 500 bins from which to compute a mean Z_{DR} and the standard deviation must be less than 0.5 dB. Finally, the RPG computes an average Z_{DR} from the estimated Z_{DR} for the current volume scan and the past 11 volume scans.

The dry snow Z_{DR} bias estimates, along with the light rain bias estimates are saved in an RPG system log file and archived every 8 hours at the NCDC which the ROC routinely retrieves. The Applications Branch, using MATLAB code, extracts the dry snow-based estimates from the archived log files to develop longer-term averages. As with the light rain method, an average of estimated system Z_{DR} bias for contiguous periods of 3 to 6 hours are tabulated for each site. A gap of up to 1 hour is permitted in computing the averages. Up to 4 estimates per day are possible. The median of all bias estimates for a month represents the monthly estimate for the system Z_{DR} bias for any given site.

3.3 Bragg Scatter

Researchers have known about optically clear air returns, initially called "angels" (Atlas 1959), since the 1950's. One type of clear air return is referred to as Bragg scatter. This return can be produced by turbulent eddies of moist air at the top of the convective boundary layer or turbulence caused by strongly sheared winds with minimal moisture and temperature discontinuities. The radar optimally detects Bragg scatter when the turbulence size scale is half the wavelength of the radar beam. For the WSR-88D, this would be half of ~10 cm or ~5 cm. (See Figure 2.) More recently Melnikov et al. (2011) demonstrated that under favorable conditions the WSR-88D can detect Bragg scatter. Moreover, the WSR-88D's dual-polarization parameters allow one to uniquely identify regions of Bragg scatter free of contamination from biota, precipitation, or ground clutter. Contamination-free Bragg scatter has the property that Z_{DR} is inherently ~0 dB. Any deviation from 0 dB reflects a system Z_{DR} bias. To detect regions of Bragg scatter Melnikov used the NSSL's KOUN test bed WSR-88D in a special stationary scanning mode that allowed him to average as many as 768 pulses and construct detailed range height plots.

In early summer 2013, Melnikov suggested that an operational WSR-88D, using existing volume coverage patterns (VCPs), might also detect Bragg scatter. Hoban (2013), Cunningham (2013), and Zittel (2014) describe such an automated process.

Currently, the algorithm runs entirely in MATLAB focusing on a 2-hour window from 17-19 UTC daily for all WSR-88Ds. VCPs are limited to 32 and 21, the former being the short pulse clear-air VCP and the latter a precipitation mode VCP for monitoring precipitation distant from the radar. Candidate values of Z_{DR} from Bragg scatter are accumulated in a histogram over the two hour window and a modal value obtained. Only elevation angles between 2.5° and 4.5°, inclusive, and ranges between 10 and 80 km are considered. Range resolution of the WSR-88D is 0.25 km. For a radar bin to be considered to have Bragg scatter, reflectivity must be < 10 dBZ, SNR must be between -5 dB and + 15 dB, RHO_{HV} must be > 0.98 and < 1.05. Additionally, the absolute value of velocity must be > 2.0 m s^{-1}, and spectrum width > 0 m s^{-1} to mitigate clutter contamination. At 18:04 UTC on November 10, 2013 a ring of Bragg scatter at 2.5° elevation from the Milwaukee, WI radar (KMKX) is illustrated in Figure 3.

Two statistical filters are applied to the Z_{DR} histogram. It must have at least 10,000 data points to insure a smooth distribution and the Inter-Quartile Range (IQR) must be < 0.9 dB to mitigate contamination from biota. That is, it must have high kurtosis and not be skewed.

A histogram of all reflectivity values in the space and time domain is tabulated. The 90th percentile for this histogram must be ≤ -3 dBZ. This reduces the likelihood of contamination from light precipitation, especially snow in winter.

Only one estimate per day can be obtained currently and the time period sampled may not be optimal fleetwide. The median of all days with an estimate of the system Z_{DR} bias from Bragg scatter is taken to be the bias in any given month. In the spring of 2015, a new WSR-88D software release will allow for continuous computation of Bragg scatter estimated Z_{DR} bias. Estimates from this method will then be extracted from the RPG system status log file similar to the light rain and dry snow methods.

4. SEASONAL / GEOGRAPHICAL AVAILABILITY

To understand the availability (likelihood of obtaining) estimates from each method we have analyzed a year of data from the contiguous 48 states, Puerto Rico, Alaska, and Hawaii. (By no means do the authors intend this analysis to represent climatology.) Figure 4 shows major United States (U.S.) geographical features referenced in this section and Figure 5 shows the International Civil Aviation Organization (ICAO) designation minus the initial letter (K for the lower 48 states, P for Hawaii and Alaska, or T for Puerto

Rico). Geographical maps for each method for each month show how many observations were obtained. A total of 36 charts were produced. Here we present only 12 (figures 6-17); for each method we show the maps for October 2013, January 2014, April 2014, and July 2014. The complete set of charts may be found at http://www.roc.noaa.gov/WSR88D/Applications/AppsPapers.aspx and by clicking on the Supplemental maps link for this paper.

Besides having the correct type of weather, estimates from each method are dependent on radar availability which has not been considered in this analysis. However, for Bragg scatter it is appropriate to consider the frequency with which sites run a VCP required by this method. This method also utilizes the ROC Level II data server which for certain sites and certain months did not always acquire complete volume scans and were unusable. Those volume scans were omitted from the analysis and also affect the availability of Bragg scatter estimates.

Sites for which the radar hardware is remote from a forecast office, such as certain western U.S. sites or those operated by the Federal Aviation Administration (Puerto Rico, Alaska, and Hawaii), have two separate processing streams, channel 1 or channel 2. The frequency of occurrence is shown for each channel as two boxes one below the other. The appropriate frequency is the sum of the numbers in each box. However, each channel has its own bias and must be considered separately. We presume that the greater the number of estimates, the greater the reliability of the monthly estimate obtained.

4.1 Light Rain

Figures 6-9 show the sites for which we were able to compute a light rain estimate and the frequency of the estimates. All four figures indicate both a greater frequency of occurrence and greater availability for the eastern contiguous U.S. than for the western contiguous U.S. January (Figure 7) has the fewest number of sites with Z_{DR} bias estimates with those sites being limited to the east coast and states with the Appalachian Mountains. Most sites have 10 or fewer estimates. Only sites in Florida have more than 10 estimates for the month and only Key West (KBYX) has more than 20. Puerto Rico (PR), somewhat surprisingly, has only 9 estimates as do the Hawaiian Islands (HI) on average. The Alaska (AK) sites have no estimates. Both October (Figure 6) and April (Figure 8) have similar patterns. States west of the Great Plains are lacking any estimates. Sites reporting more than 10 estimates are mostly east of the Mississippi River in April but also extend into Texas in October. Three sites ringing the Gulf of Mexico have more than 20 estimates and PR has nearly 40 estimates. Light rain estimates are most plentiful for July with only a few western sites having no estimates. Numerous sites along the east coast and in the Appalachian Mountains have > 20 estimates. Fewer than 10 estimates are available from AK, HI, or PR, the last being a bit of a surprise. However, it is possible for these sites that the light rain method's time continuity requirement is longer than the average length of light rain events.

4.2 Dry Snow

Figures 10-13 show sites for which we were able to compute estimates of system Z_{DR} bias from dry snow. Estimates are available for nearly all sites year round. For the contiguous U.S. both April and July (Figures 12 and 13) have an abundance of sites with more than 20 estimates and for July there are several sites in the southern Rockies that have more than 40 estimates. Also, a swath of sites oriented north-south roughly following the Mississippi River has fewer than 20 estimates per site which may merely be due to natural variations in the weather. October (Figure 10) has more estimates in northern and eastern states with > 20 estimates decreasing to 10 or fewer estimates west of the Rockies. In January (Figure 11) sites with > 20 estimates are largely east of the Mississippi River or in the Pacific Northwest. Several sites in the southwestern contiguous U.S. (KEYX, KICX, KFSX, KABX, KFDX, KAMA, and KLBB) have no estimates. HI has < 10 estimates for October, April, and July. Only for January does HI have > 10 estimates at two sites, (PHKM - 13 and PHWA - 12). By contrast, PR has < 10 estimates for January, April, and July but almost 30 for October possibly due to increased tropical precipitation activity during this time of year. Regardless of season, most of the sites in AK have > 10 estimates. Many coastal sites have greater than 40 estimates and 3 sites (PACG, PAIH, and PAHG) have 70 or more. In April (Figure 12), the interior sites PAPD and PAEC have < 5 estimates.

4.3 Bragg Scatter

As mentioned in Section 3.3, this method for estimating system Z_{DR} bias was limited to a 2-hr window from 17-19 UTC due to processing time constraints using MATLAB. We discuss these results in Section 4.3.1. (See Figures 14-17.) In 4.3.2 we discuss the availability of Bragg scatter bias estimates from 17 sites from different climatic

regions in the U.S. when running continuously for the four months October 2013, January 2014, April 2014, and July 2014. Because the number of estimates is limited to 1 per day, the values in the legend have been halved for these figures.

4.3.1 2-Hour Time Window 17-19 UTC

The October 2013 map (Figure 14) shows that most of the contiguous U.S. as well as AK and HI have < 5 estimates. A few sites, mostly in the northeastern U.S. have 10 or more estimates. Many sites have no estimates at all. The January 2014 map (Figure 15), by contrast, shows many sites in the southeastern through the south central U.S. having greater than 10 observations while nearby sites and sites along the northern east coast have greater than 5. Contrast this map with the map for July 2014 (Figure 17). For July, over half the sites in the contiguous U.S. have no estimates while most of the remaining sites have 5 or fewer estimates including AK and HI. This seems to be counterintuitive in that there is more moisture and surface heating in July than in January. Two factors limit detection in July: 1) contamination from biota (most probably insects) and; 2) sites using a VCP other than 21 or 32. We surmise that in January, there is just enough moisture and surface heating without contamination from biota to allow Bragg scatter to be detected in the southeastern U.S. and adjacent states. Figure 16 (April 2014) shows most sites have 5 or fewer estimates from Bragg scatter. A few more northerly sites have > 10 estimates for April. PR (TJUA) has no estimates for any of the 4 months. Fleetwide, average usage of VCP 21 is ~17% and VCP 32 is ~32%. Table 2 shows the percent of average WSR-88D usage fleetwide of VCPs 21 and 32 for 17-19 UTC. Greatest usage of the VCPs used for Bragg scatter detection occurs in January at 78.0% while the lowest usage occurs in April with 50.7%. For each of these 4 months a Bragg scatter VCP is used > 50% of the time.

Table 2. Percent of number of volume scans used in the WSR-88D fleet for VCPs 21 and 32 for October 2013, January 2014, April 2014, and July 2014.

VCP	Oct '13	Jan '14	Apr '14	Jul '14
21	27.5	30.1	15.0	10.9
32	38.5	47.9	35.7	45.9
Sum	66.0	78.0	50.7	56.8

4.3.2 Continuous Bragg Scatter Detection

To determine the presence of Bragg-like scatter continuously, MATLAB code emulates the processing planned for the May 2015 WSR-88D software release. The same data filters are used as in the 2-hour window with the following exceptions. If data have passed the necessary filters, values of Z_{DR} are tabulated in a 12-volume running histogram. After 12 volumes the oldest data in the histogram is removed and the new data added. Any time there are at least 10,000 bins in the Z_{DR} histogram, even if there are fewer than 12 volume scans, an estimate of the system Z_{DR} bias is output. Regardless of the number of estimates per day from continuous monitoring, only 1 estimate was counted to provide a direct comparison to the number of days available from the 2-hour window estimates.

Seventeen WSR-88D sites (shown in Figure 5) were selected for their geographical diversity to determine the frequency with which Bragg scatter could be found when not restricted to an arbitrary 2-hour time window. Bar charts for the same 4 months as shown in previous figures compare the number of days with Bragg scatter system Z_{DR} bias estimates from the 2-hour and the continuous (24/7) methods. Table 3 provides a list of the site names and their ICAO designation. The table and bar charts are roughly organized from drier (e.g. KIWA) to wetter (e.g. TJUA).

Table 3. List of the 17 WSR-88D sites used to look for Bragg scatter continuously during October 2013, January 2014, April 2014, and July 2014.

ICAO	**WSR-88D Site**
KIWA	Phoenix, AZ
KOTX	Spokane, WA
KEYX	Edwards AFB, CA
KUDX	Rapid City, SD
KPUX	Pueblo, CO
KUEX	Hastings, NE
KTLX	Oklahoma City, OK
KILN	Cincinnati, OH
KLGX	Langley Hill, WA
KBHX	Eureka, CA
KLCH	Lake Charles, LA
KJGX	Robbins AFB, GA
KGRR	Grand Rapids, MI
KCBW	Caribou, ME
PAIH	Middleton, AK
PHMO	Molokai, HI
TJUA	San Juan, PR

All four months (Figures 18-21) show that continuously monitoring for Bragg scatter yields

many more days than just using a 2-hour window (713 vs. 192). Regardless of sampling method, July (Figure 21) has the fewest number of days with Bragg scatter estimates (97 for continuous monitoring and 13 for the 2-hour window) while January (Figure 19) has the greatest number of days with estimates (223 and 70, respectively). Uniformly across the 17 sites, April (Figure 20) shows the greatest consistency in providing system Z_{DR} bias estimates. Not surprisingly, KIWA has the fewest estimates regardless of month despite using VCPs 21 and 32 routinely (> 60% of all volume scans). However, in July VCP 212 was used ~90% of the time and may be tied to the start of the North American Monsoon season. (We note that almost 25% of the volume scans were unusable in July.) In contrast, TJUA had no Bragg scatter Z_{DR} bias estimates when limited to a 2-hour window but had 6, 24, 16, and 10 daily estimates for October, January, April, and July, respectively, when monitoring for Bragg scatter continuously. TJUA uses VCPs 21 and 32 almost exclusively. There might have been more days with estimates in July except that ~50% of the volume scans were unusable.

KIWA, KUDX, KTLX, and KLGX had no July days with estimates from continuously monitored Bragg scatter. For KUDX, VCPs 21 and 32 were used about 20% of the time. For KTLX, VCPs 21 and 32 were used > 25% of the time but nearly 35% of the volume scans were unusable. For KLGX, nearly 95% of the volume scans were unusable.

5. OPERATIONAL USE OF WEATHER-BASED Z_{DR} BIAS ESTIMATES

During the fall of 2014, the ROC began routinely generating shade charts for each WSR-88D such as shown in Figure 22 for KCBW. Each chart consists of a year's record of estimated system Z_{DR} bias for each of the 3 methods. The top panel displays the estimates from light rain, the middle panel displays the estimates from dry snow, and the bottom panel displays the estimates from Bragg scatter within the 2-hour window previously discussed. The charts are updated monthly. Weekly medians for each method are shaded to show either a high bias (red) or a low bias (blue). (A comprehensive discussion of construction of the charts may be found in Zittel et al. 2014.) The short-period estimates (either in 6 hour blocks for light rain and dry snow or daily for Bragg scatter) are plotted on top of the shaded areas. ROC staff consults with operational staff at those WSR-88D sites whose shade charts indicate a bias exceeding ± 0.2 dB in the same direction for all three methods.

Although the dry snow method provides the greatest number of estimates, it is seen to have the greatest variability in short-term estimates of the 3 methods. The light rain method is slightly less noisy than the dry snow method but does not provide estimates nearly as often. The Bragg scatter method appears fairly stable but is limited to only a daily estimate. Such variability necessitates that one assess bias from many estimates over a long length of time. The authors recommend at least one to three months of estimates are required before a safe assessment of overall bias can be determined.

A companion graph (Figure 23) compares the system's hardware-based estimated bias (ZDRB) to the median bias from the combined meteorological methods. A larger bias is seen when the hardware-based estimate falls outside of the gray envelope (which is ± 0.2 dB around the median of the meteorological methods). If only one method is available, that method is taken to be representative of all the meteorological methods. Thus, single-method estimates with contamination may result in outliers. Notice the singular jump in the meteorological-based estimate of system Z_{DR} bias in early March. This jump does not fit either the previous or later ZDRB estimates. Looking back to the shade chart (Figure 22), we can note the large jump in Bragg scatter at this time. Also note that Bragg scatter is the only method contributing to this period, resulting in the outlier jump in the ZDRB chart. Having estimates from multiple methods over time greatly assist in identifying such outliers. Understanding the limitations of the meteorological estimates both in reliability and in geographical and seasonal availability is crucial to interpretation of shade and ZDRB charts. A proper interpretation of the charts is needed when contacting sites for potential corrections to Z_{DR} bias.

6. SUMMARY

Three methods for determining system Z_{DR} bias estimates from meteorological returns have been described along with seasonal and geographical tendencies towards availability for 4 representative months (Oct '13, Jan '14, Apr '14, and Jul '14) for one year. The first method (light rain) looks at values of Z_{DR} from strong SNR from echoes ~20-30 dBZ and well below the melting layer. The second method (dry snow) looks at values of Z_{DR} from strong SNR in a layer immediately above the melting layer. The third method (Bragg scatter) looks for values of Z_{DR} from weak signal in clear air. Data and statistical filters for this method

mitigate contamination from ground clutter, biota, and light precipitation.

Estimates from dry snow occur most often in all regions of the contiguous U.S., Hawaii, Alaska, and Puerto Rico but exhibit large variance in values even within the same weather event. Estimates from the light rain method are most frequent in the eastern half of the contiguous U.S. but spreads into the southwestern U.S. by July. January's estimates are sparsest. Light rain bias estimates are not nearly as noisy as the dry snow estimates but still require averaging to reduce the variance. Estimates from the Bragg scatter method, when restricted to a fixed 2-hour window (17-19 UTC), are severely limited with the southeastern contiguous U.S. having the greatest number of estimates in January. Continuous sampling of 17 climatologically diverse sites increases the number of Z_{DR} system bias estimates nearly 4-fold compared to the 2-hour window.

System Z_{DR} bias estimates from the 3 methods are being provided operationally to field sites. However, a few system Z_{DR} bias estimates contaminated by weather can cause a WSR-88D to be judged to be in need of calibration. Tendencies over at least a month from preferably more than one method should be used to gauge the quality of Z_{DR} data from any given radar.

7. ACKNOWLEDGMENTS

The authors thank their colleagues within the ROC for their stimulating discussions regarding the development of this work and especially the reviewers for suggesting improvements to this paper.

REFERENCES

Atlas, David, 1959: METEROROLOGICAL "ANGEL" ECHOES. *J. Meteor.*, **16**, 6–11.

Bringi, V. N., and V. Chandrasekar, 2001: Physically based parametric rain rate estimation algorithms. *Polarimetric Doppler Weather Radar: Principles and Applications*. Cambridge University Press, 636 pp.

Cunningham, J. G., W. D. Zittel, R. R. Lee and R. L. Ice, 2013, Methods for identifying systematic differential reflectivity (Zdr) biases on the operational WSR-88D network, *36th Conference on Radar Meteorology.* [Available at http://ams.confex.com/ams/36Radar/webprogram/Manuscript/Paper228792/JCunningham_36th RadarConf_9B5.pdf.]

Giangrande, S. E., J. M. Krause, and A. V. Ryzhkov, 2008: Automatic designation of the melting layer with a polarimetric prototype of the WSR-88D radar. *J. Appl. Meteor. Climatol.,* 47, 1354–1364.

Hyang Suk Park, A. V. Ryzhkov, D. S. Zrnić, and Kyung-Eak Kim, 2009: The Hydrometeor Classification Algorithm for the Polarimetric WSR-88D: Description and Application to an MCS. *Wea. Forecasting*, **24**, 730–748. doi: http://dx.doi.org/10.1175/2008WAF2222205.1

Ice, R. L., A. K. Heck and J. G. Cunningham, 2013: Polarimetric weather radar calibration – engineering challenges, *36th Conference on Radar Meteorology,* Breckenridge, CO. Amer. Meteor. Soc. [Available online at http://ams.confex.com/ams/36Radar/webprogram/Paper228789.html.]

Ice, R. L., A. K. Heck, J. G. Cunningham and W. D. Zittel, 2014: Challenges of polarimetric weather radar calibration, *8th European Conference on Radar and Hydrometeorology,* Garmisch-Partenkirchen, Germany.

Melnikov, Valery M., Richard J. Doviak, Dusan S. Zrnić, David. J. Stensrud, 2011: Mapping Bragg Scatter with a Polarimetric WSR-88D. *J. Atmos. Oceanic Technol.*, **28**, 1273–1285.

Ottersten, H., 1969: Atmospheric structure and radar backscattering in clear air. *Radio Sci.*, **4**, 1179-1193.

Ryzhkov, A. V., S. E. Giangrande, V. M. Melnikov, and T. J. Schuur, 2005: Calibration Issues of Dual-Polarization Radar Measurements. *J. Atmos. Oceanic Technol.*, **22**, 1138–1155. doi: http://dx.doi.org/10.1175/JTECH1772.1

Schuur, T. J., A. V. Ryzhkov, and D. S. Zrnić, 2001: A statistical analysis of 2D-video-disdrometer data: impact on polarimetric rainfall estimation. Preprints, *30th International Conference on Radar Meteorology,* Munich, Germany. Amer. Meteor. Soc.

Schuur, T. J., A. V. Ryzhkov, and D. R. Clabo, 2005: Climatological analysis of DSDs in Oklahoma as revealed by 2D-video disdrometer and polarimetric WSR-88D radar. Preprints, *32nd Conference on Radar Meteorology,* Albuquerque, NM. Amer. Meteor. Soc.

Straka, J. M., D. S. Zrnić, and A. V. Ryzhkov, 2000: Bulk hydrometeor classification and quantification using polarimetric radar data: synthesis of relations. *J. Appl. Meteor.*, **39**, 1341-1372.

Thompson, E. J., S. A. Rutledge, B. Dolan, V. Chandrasekar, and B. L. Cheong, 2014: A dual-polarization radar hydrometeor classification algorithm for winter precipitation. *J. Atmos. Oceanic Technol.,* **31**, 1457-1481. doi: 10.1175/JTECH-D-13-00119.1

Zittel, W. D., J. G. Cunningham, R. R. Lee, L. Richardson, R. L. Ice and V. Melnikov, 2014, Use of Hydrometeors, Bragg Scatter, and Sun Spikes to Determine System Z_{DR} Biases in the WSR-88D Fleet, *8th European Conference on Radar in Meteorology and Hydrology.*

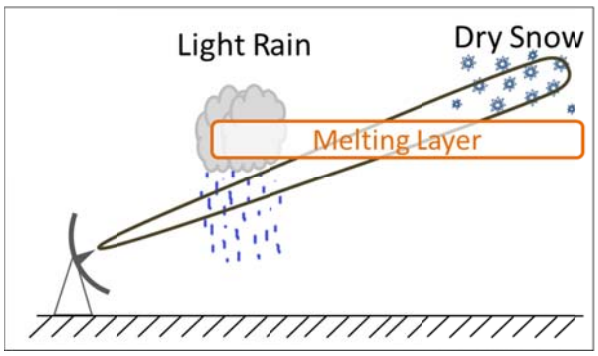

Figure 1. Schematic shows regions where estimates of system bias from light rain (below Melting Layer) and dry snow (above Melting Layer) are tabulated.

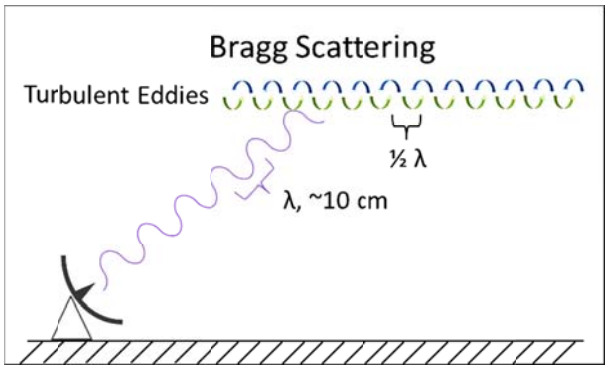

Figure 2. Schematic shows relationship of scale of turbulent eddies detected by the WSR-88D relative to its wavelength. Height at which eddies are detected is assumed to be less than 5 km.

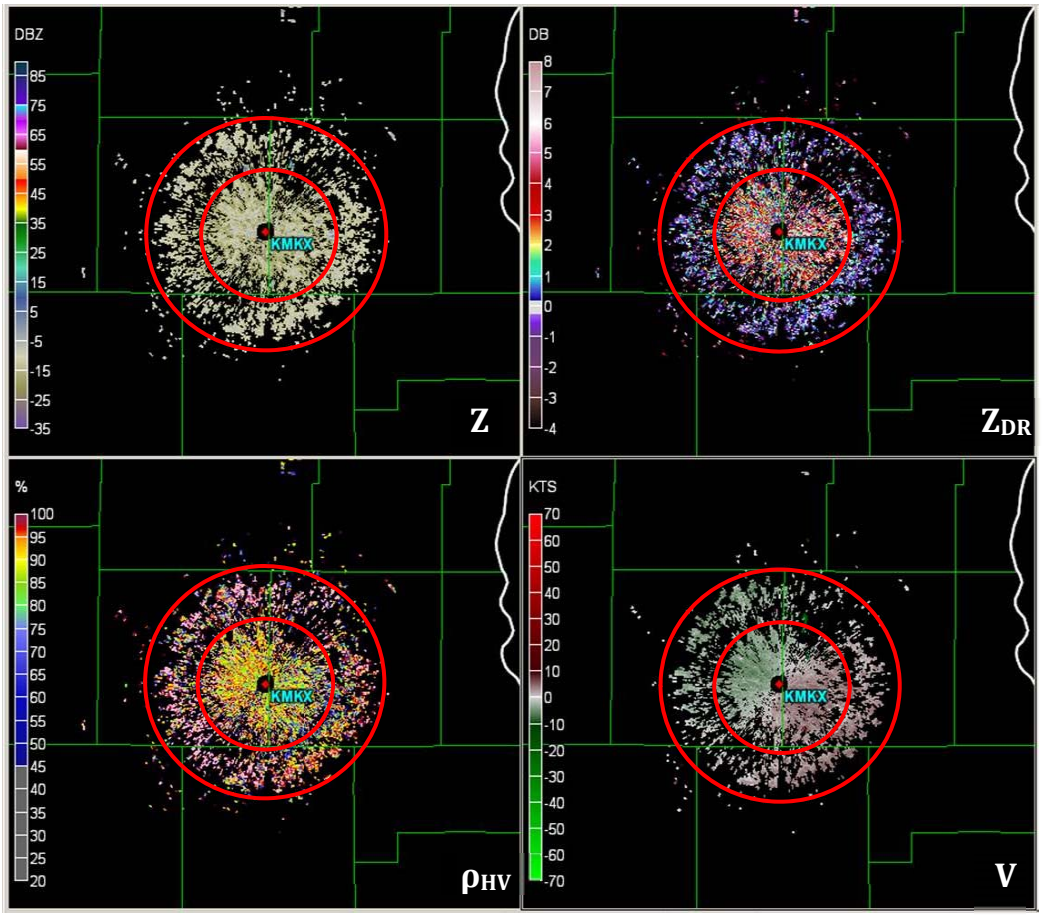

Figure 3. This figure shows type of echo returns expected from clear air Bragg scatter (area between the red rings. Reflectivity (Z) is shown in the upper left panel, differential reflectivity (Z_{DR}) is shown in the upper right panel, velocity (V) is shown in the lower right panel, and correlation coefficient (ρ_{HV}) is shown in the lower left panel. Site is Milwaukee, WI (KMKX) from November 10, 2013 at 18:04 UTC, 2.5° elevation.

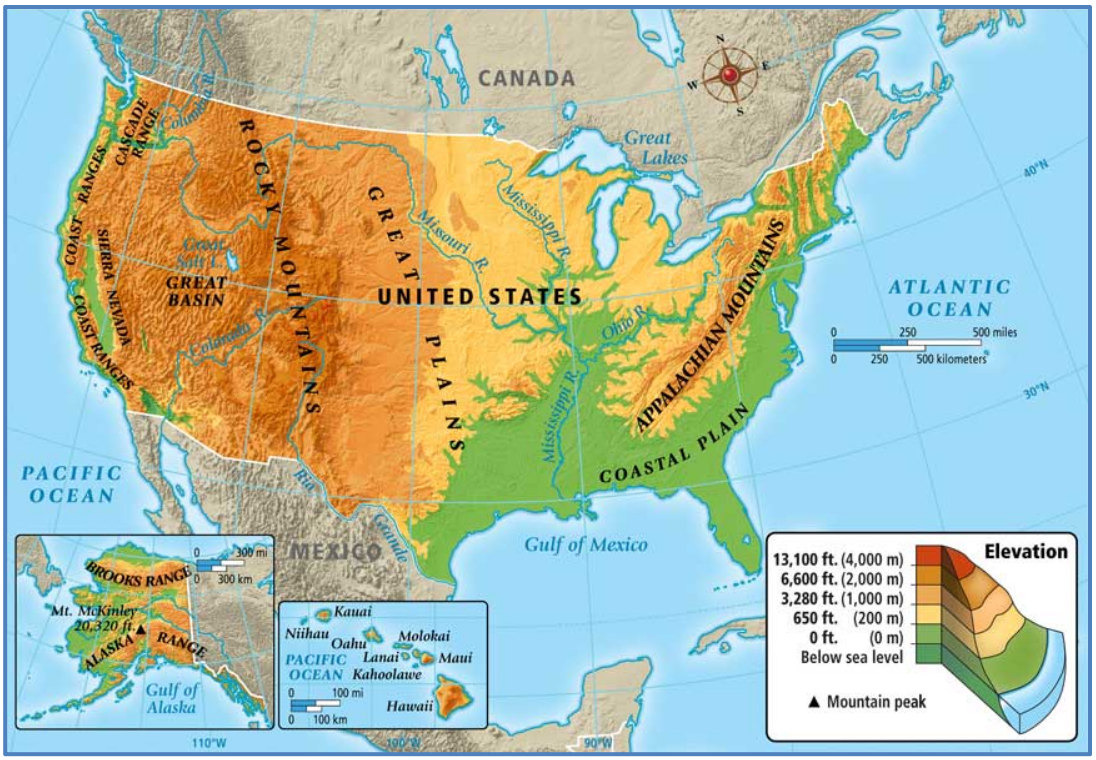

Figure 4. Physical geography map of the contiguous United States, Alaska and Hawaii with major geographical features labeled. Used with permission from Engrade (McGraw-Hill Education).

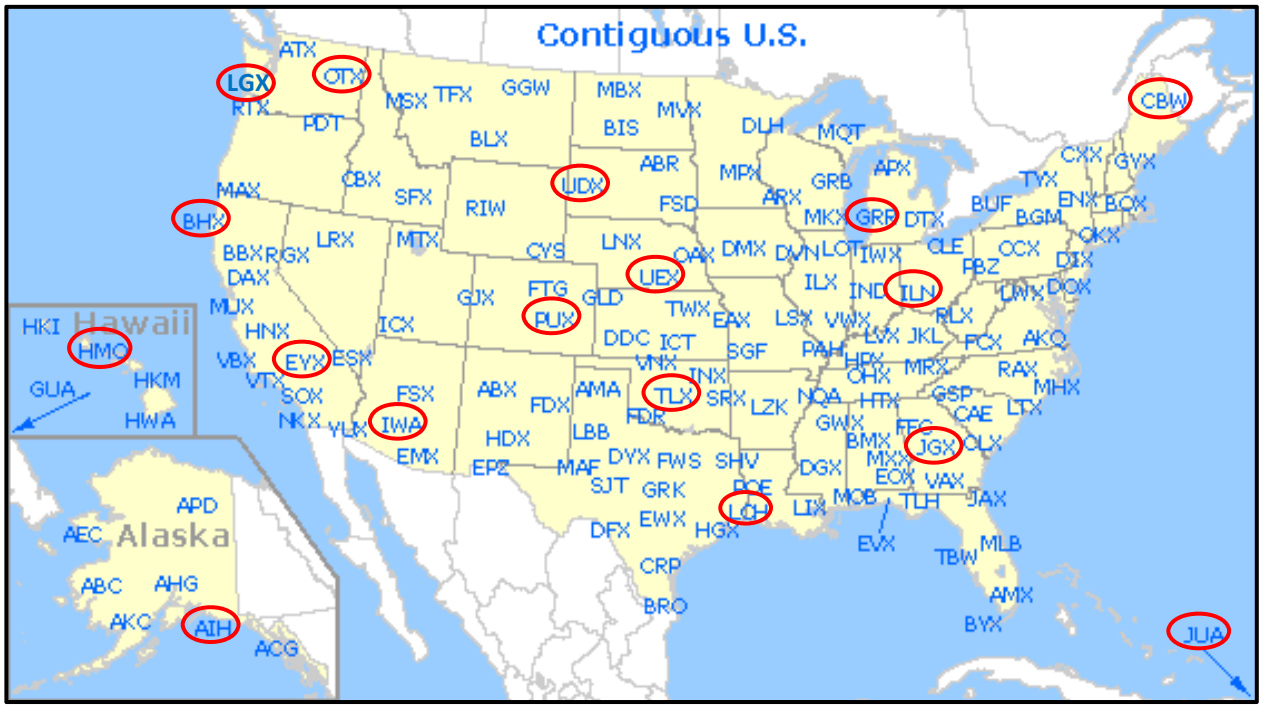

Figure 5. Map of Contiguous United States, Hawaii, and Alaska showing the relative locations of WSR-88D sites. San Juan, Puerto Rico (JUA) is just off the map. Red-circled sites were used to determine availability of system Z_{DR} bias estimates from Bragg scatter when monitored continuously. Map reproduced with permission from NCAR/UCAR.

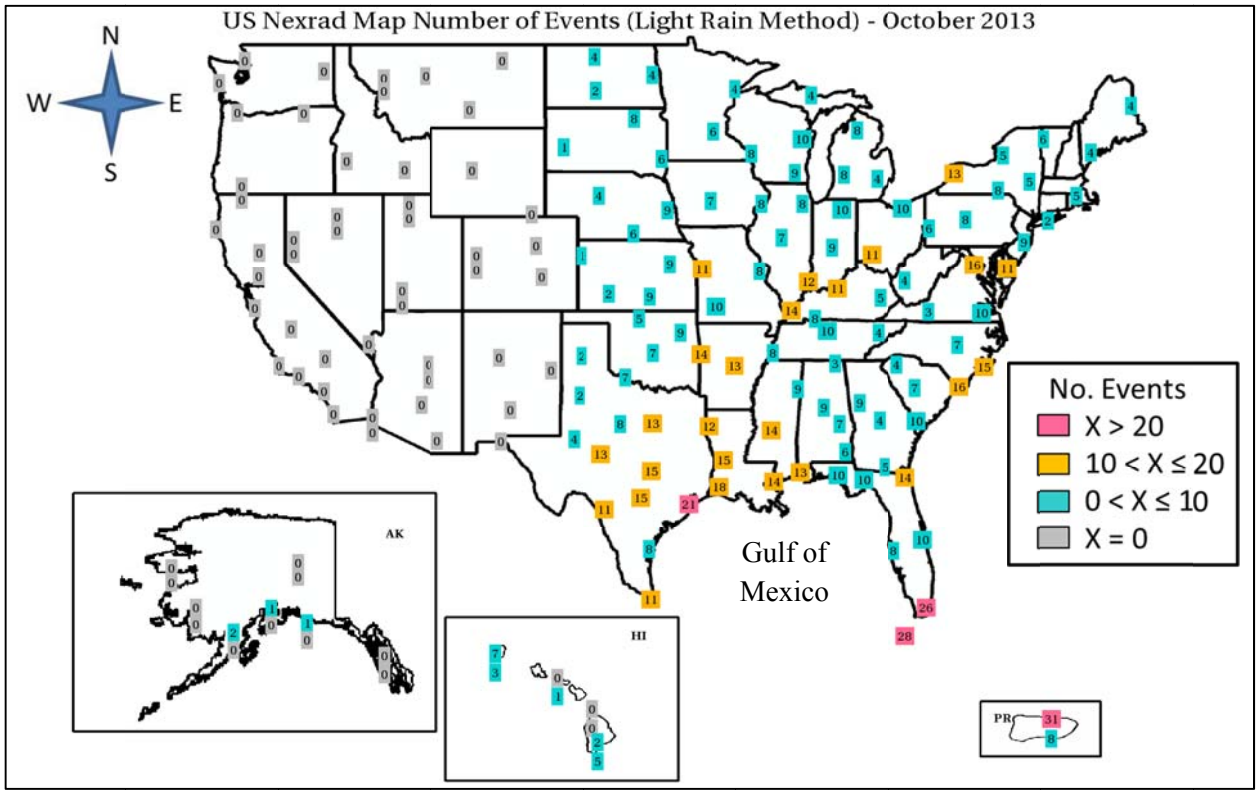

Figure 6. Map of the contiguous United States, Alaska, Hawaii, and Puerto Rico showing the number of estimates of system Z_{DR} bias from the light rain method for October 2013 for each WSR-88D. Magenta boxes indicate > 20 estimates, yellow boxes indicate between 11 and 20 estimates, aqua boxes show estimates between 1 and 10, and gray boxes show sites with no estimates. There are two boxes for sites with redundant RDA channels.

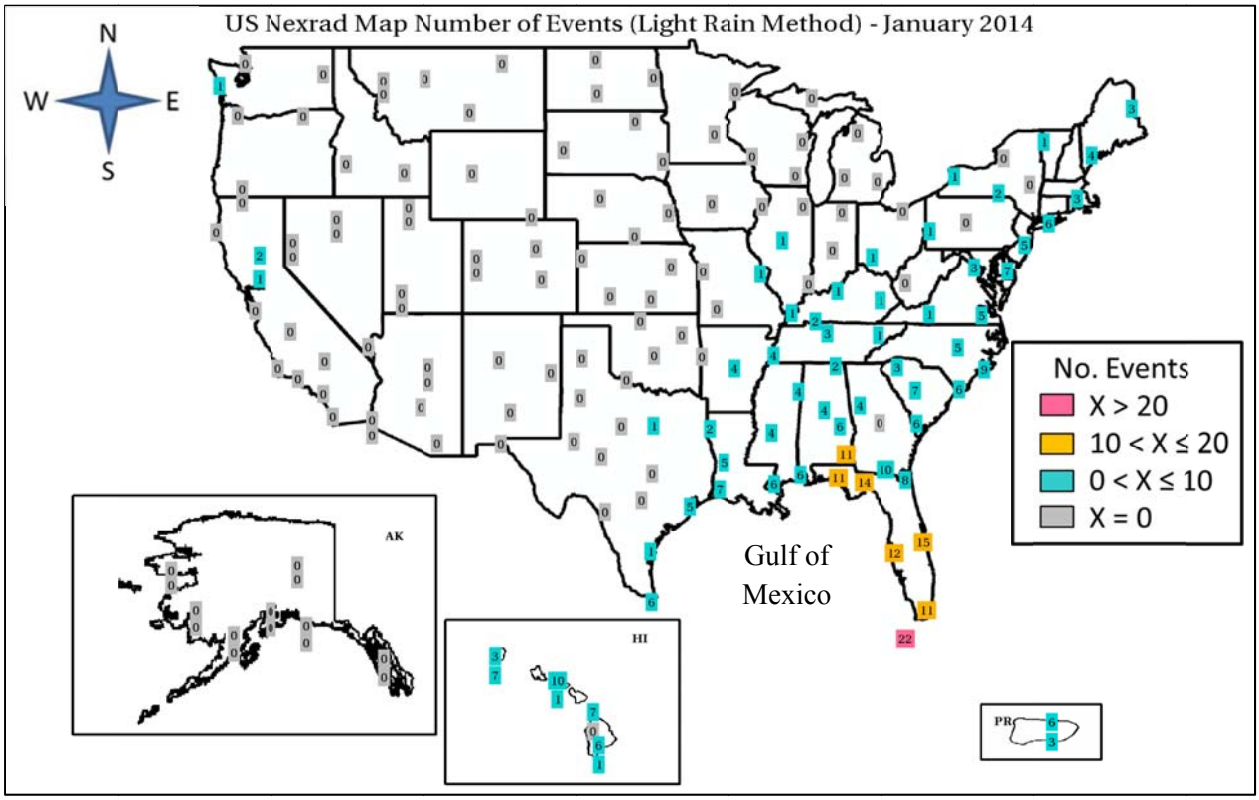

Figure 7. Same as Figure 6 but for January 2014.

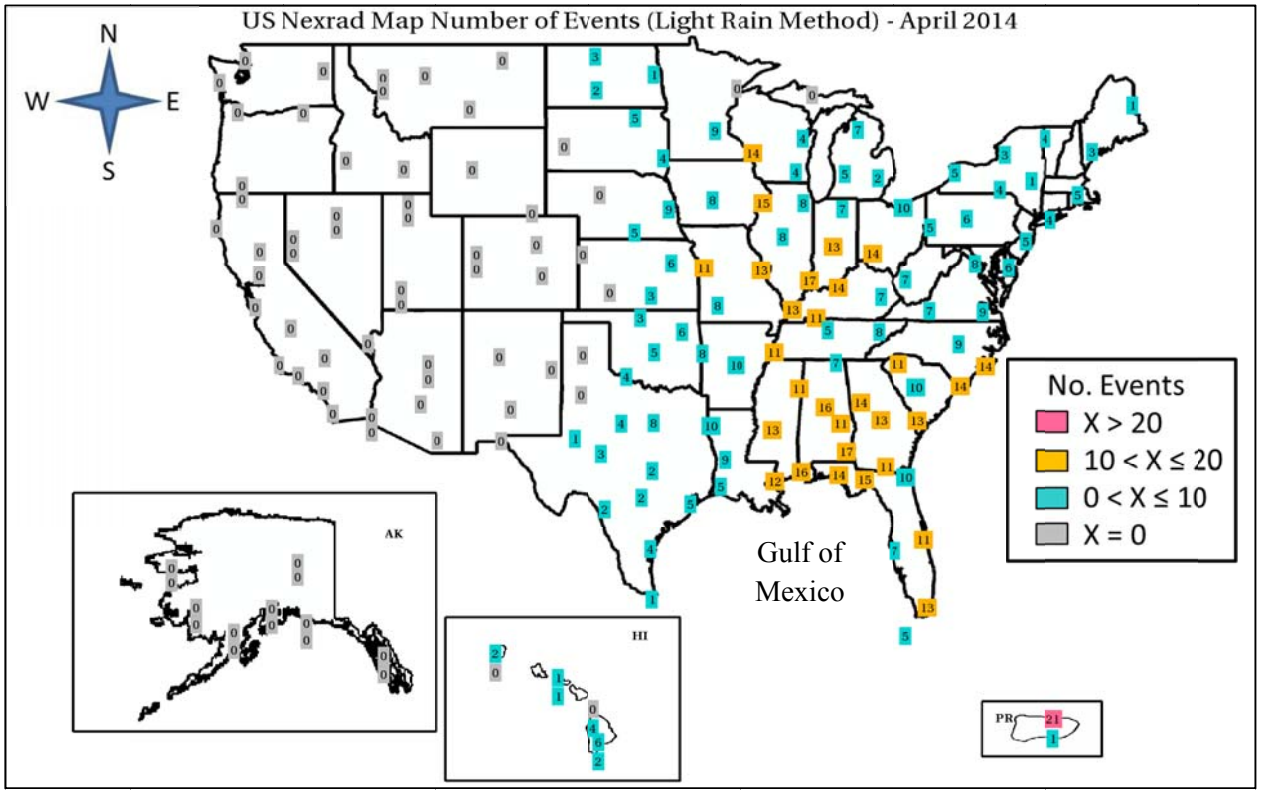

Figure 8. Same as Figure 6 but for April 2014.

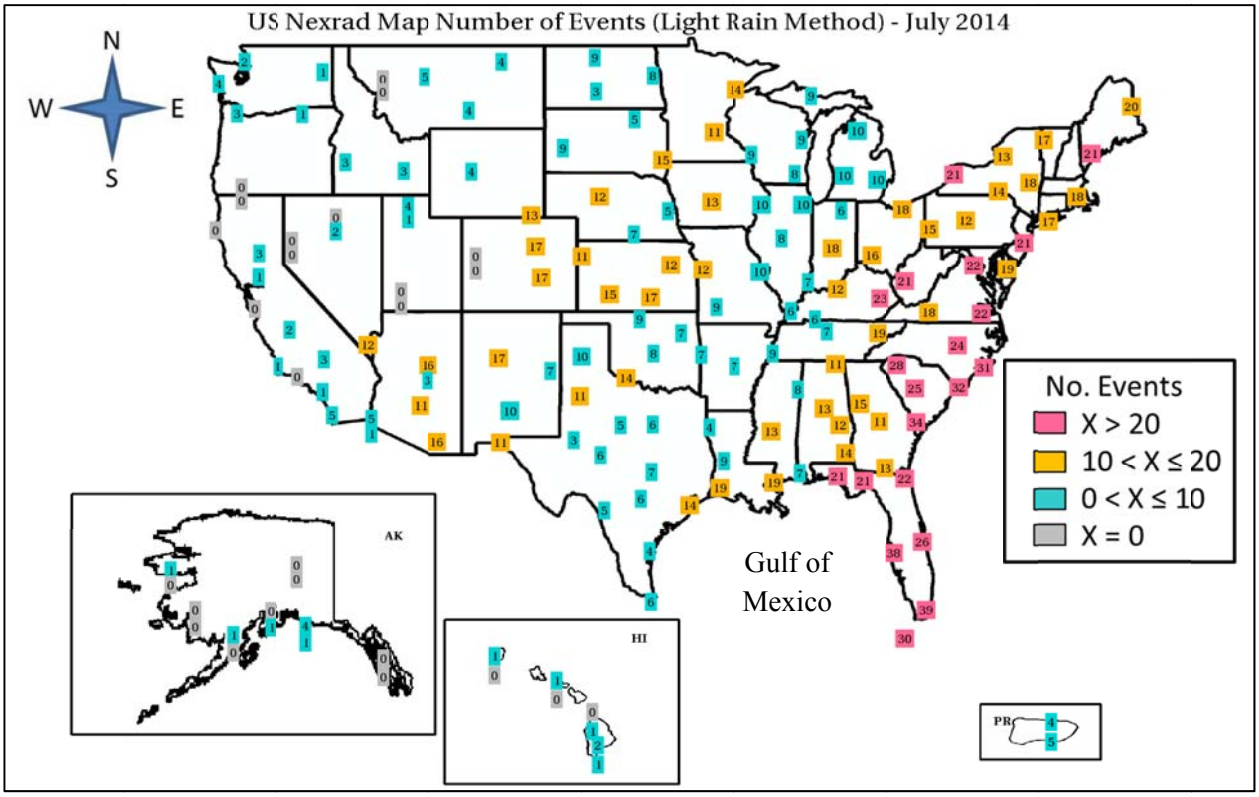

Figure 9. Same as Figure 6 but for July 2014.

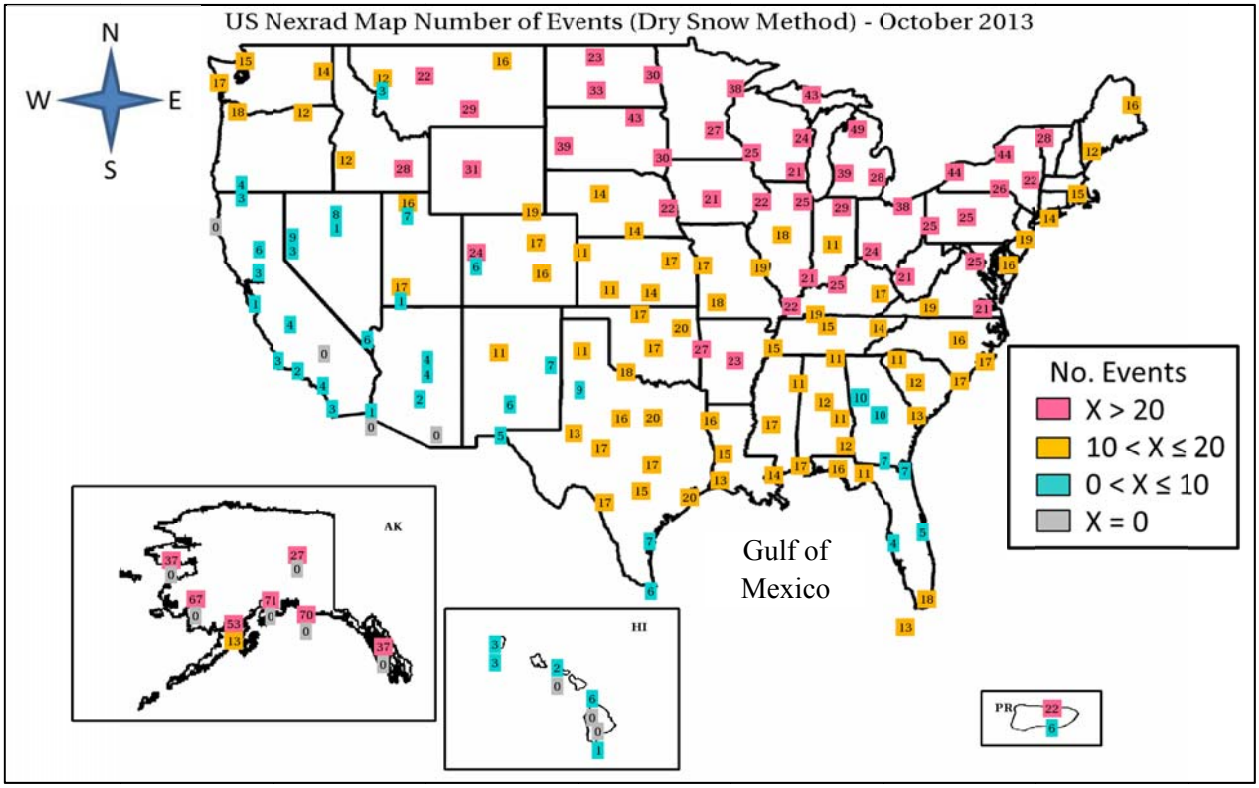

Figure 10. Same as Figure 6 but for the dry snow method.

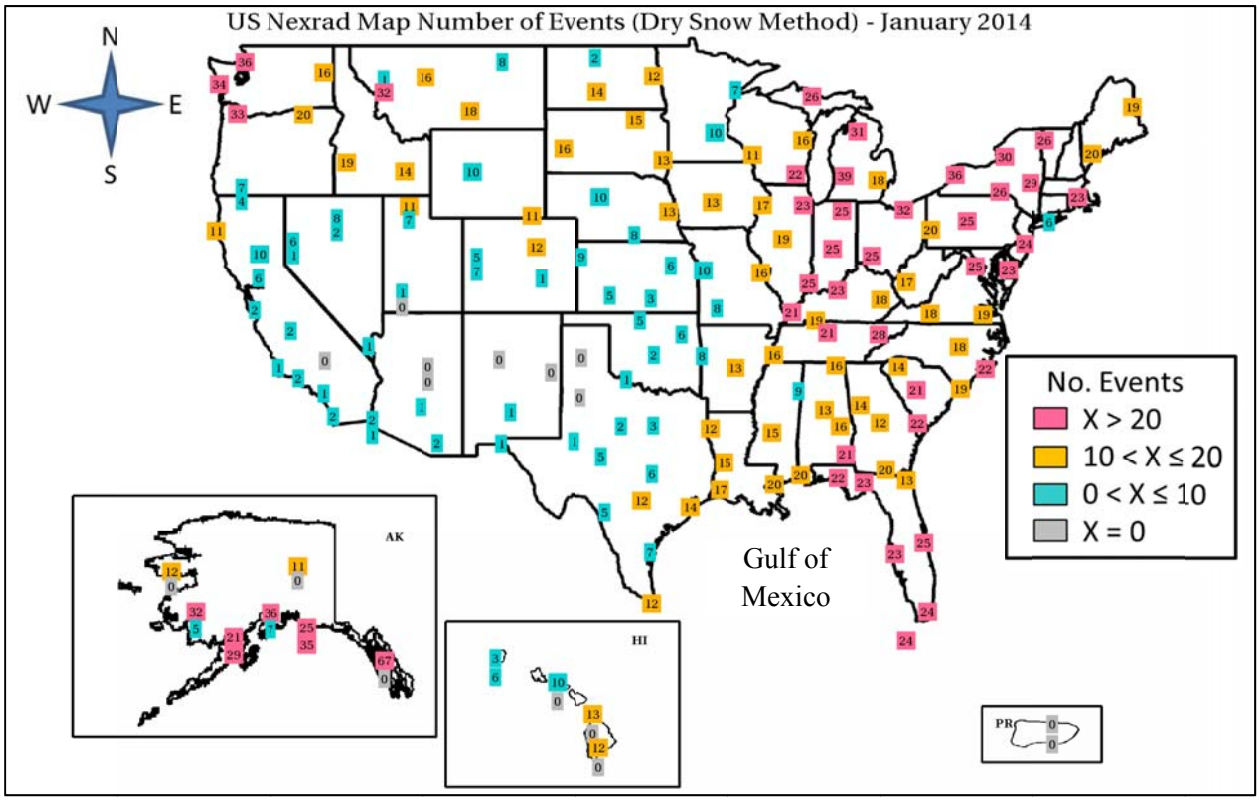

Figure 11. Same as Figure 10 but for January 2014.

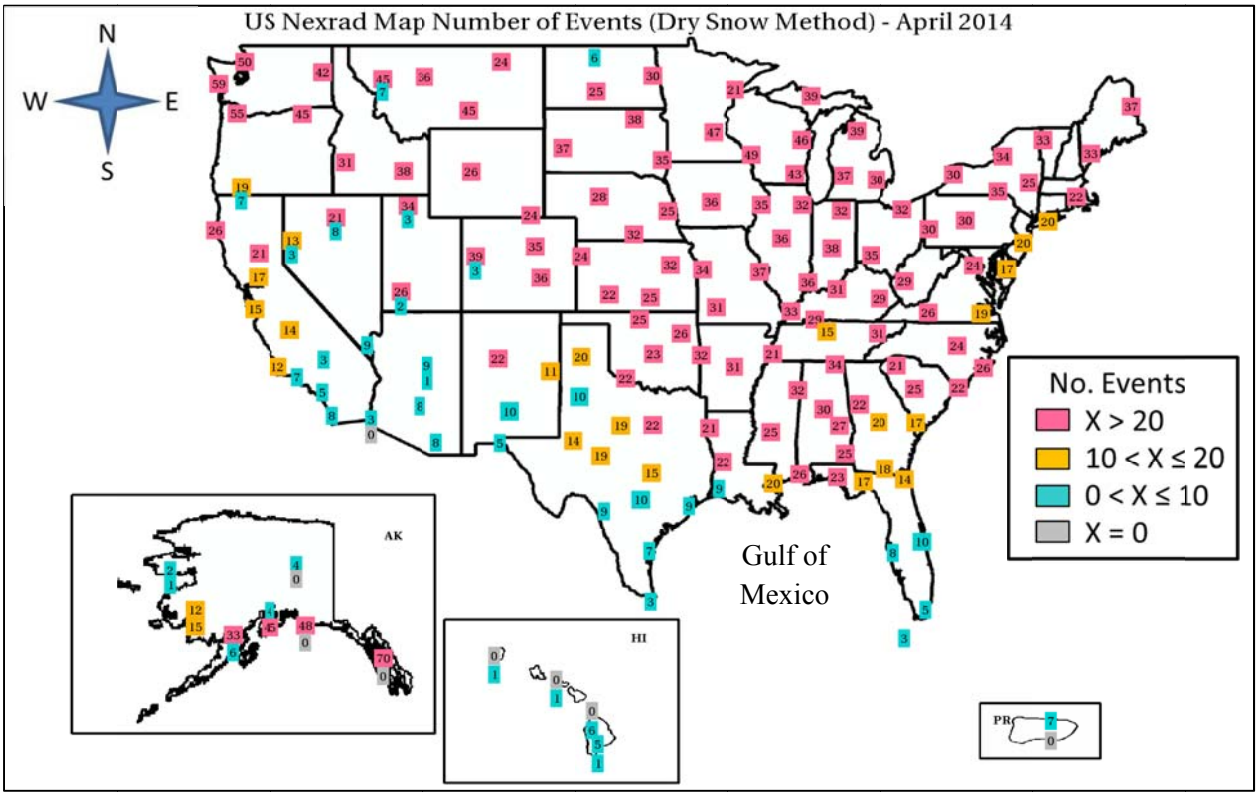

Figure 12. Same as Figure 10 but for April 2014.

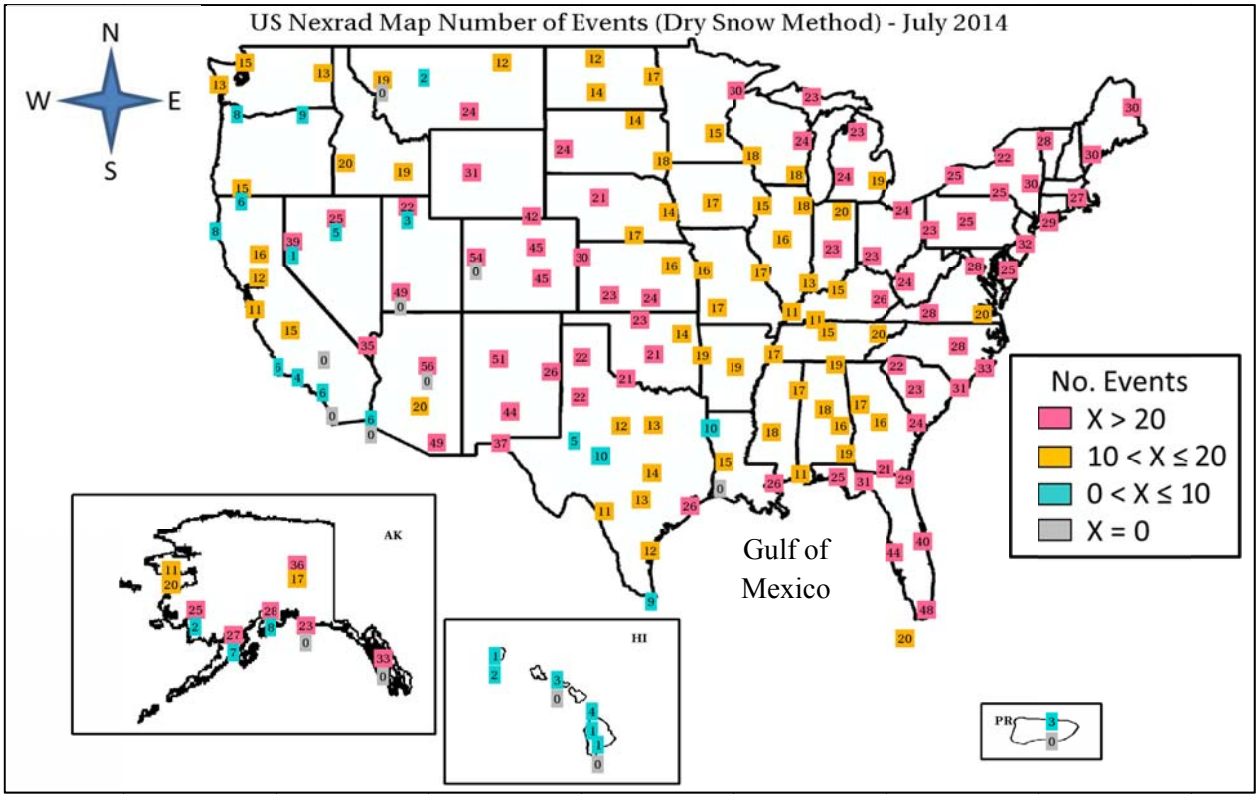

Figure 13. Same as Figure 10 but for July 2014.

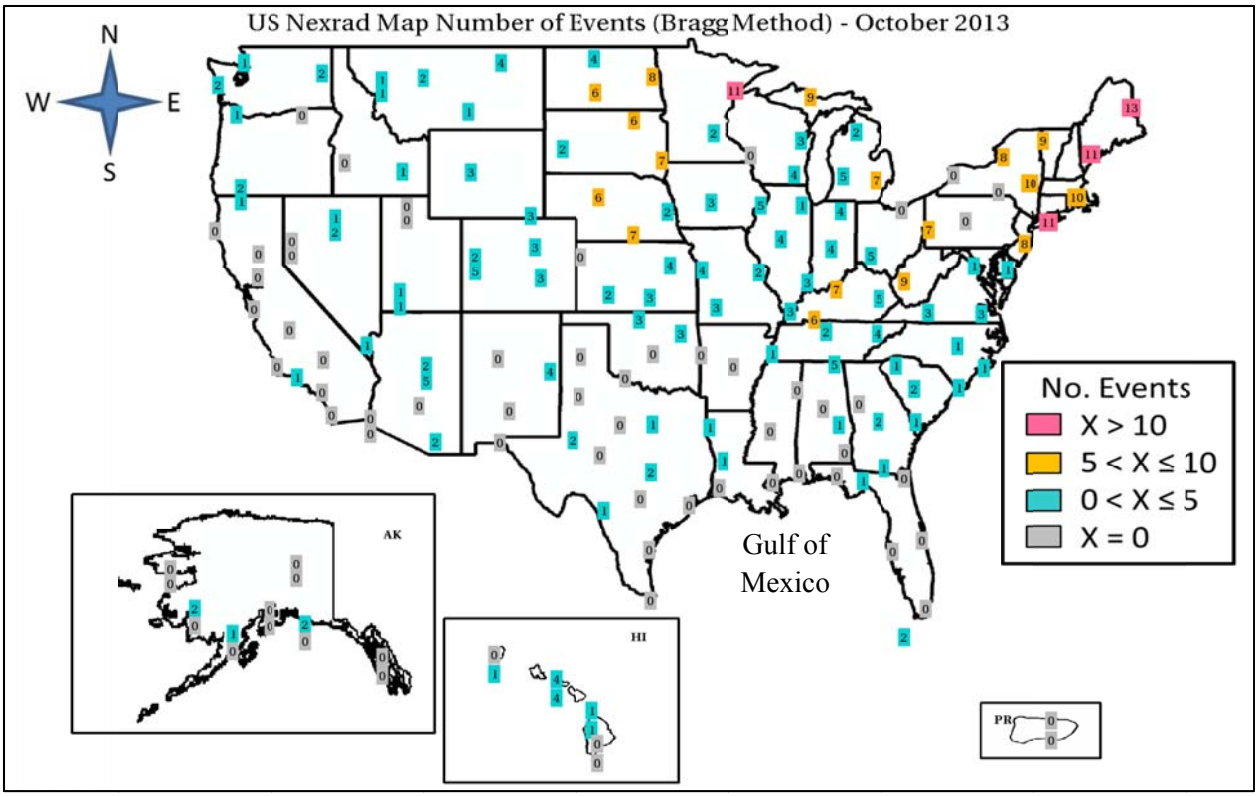

Figure 14. Same as Figure 6 but for the Bragg scatter method for October 2013. Magenta boxes indicate > 10 estimates, yellow boxes indicate between 6 and 10 estimates, aqua boxes show estimates between 1 and 5, and gray boxes show sites with no estimates. There are two boxes for sites with redundant RDA channels.

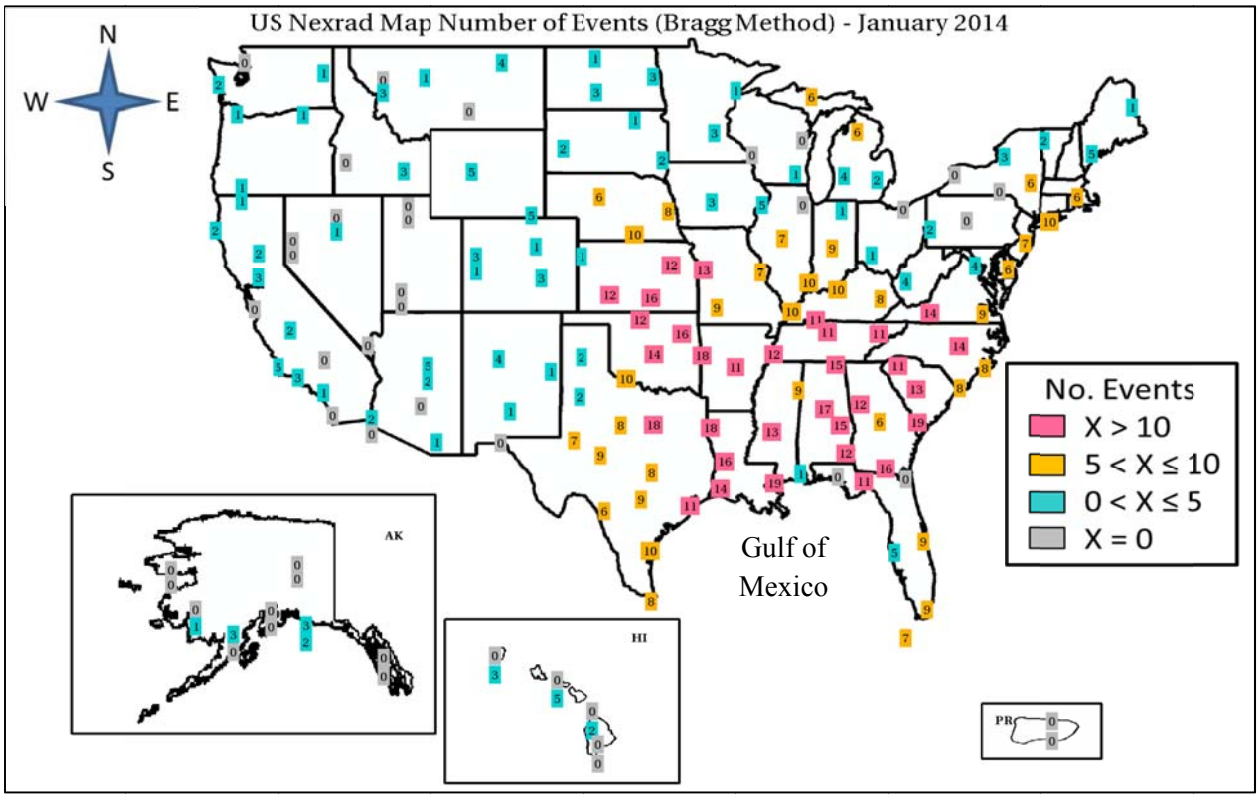

Figure 15. Same as Figure 14 but for January 2014.

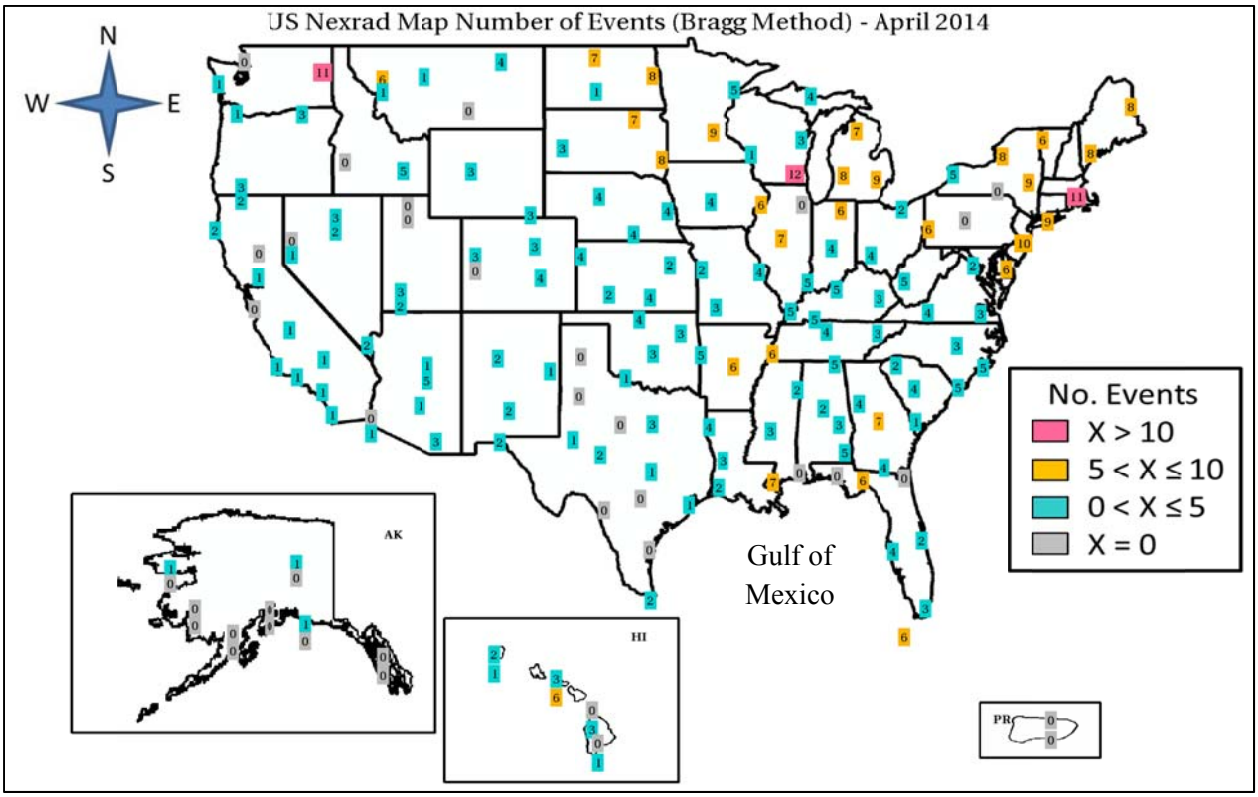

Figure 16. Same as Figure 14 but for April 2014.

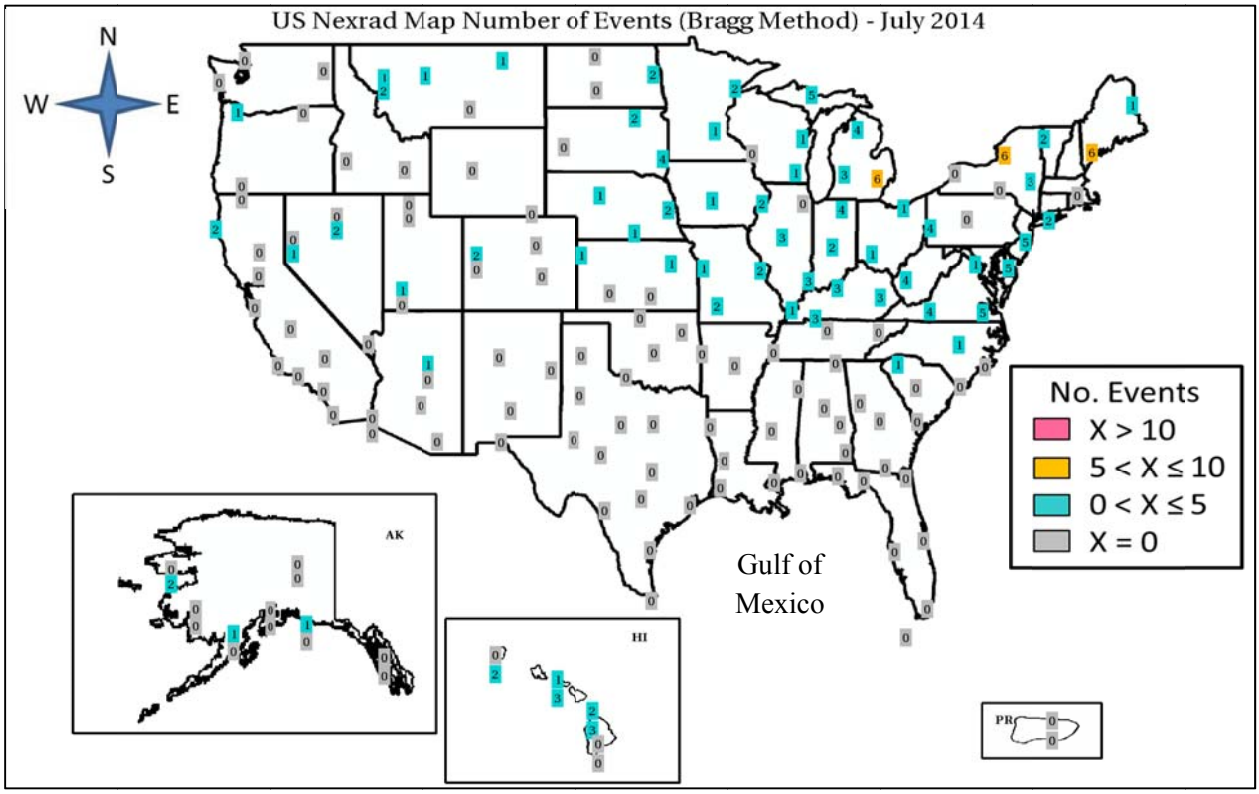

Figure 17. Same as Figure 14 but for July 2014.

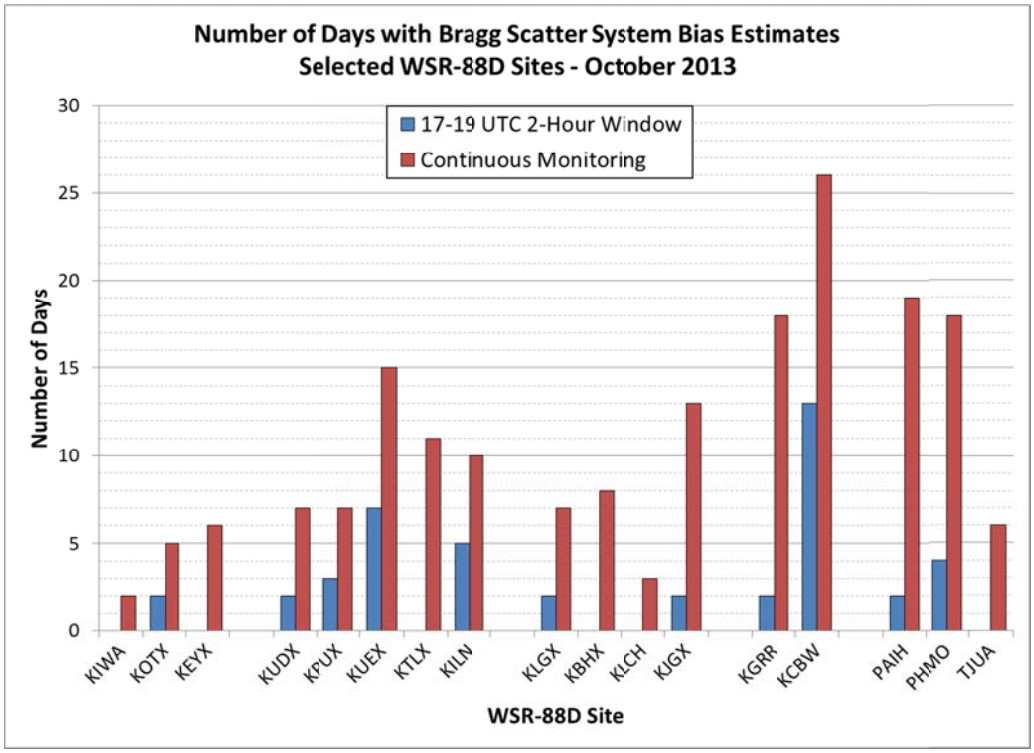

Figure 18. Bar chart comparing the number of system Z_{DR} bias estimates available from the 2-hour window (17-19 UTC, blue bars) compared to estimates available from continuous monitoring (maroon bars) for 17 climatologically diverse sites for October 2013.

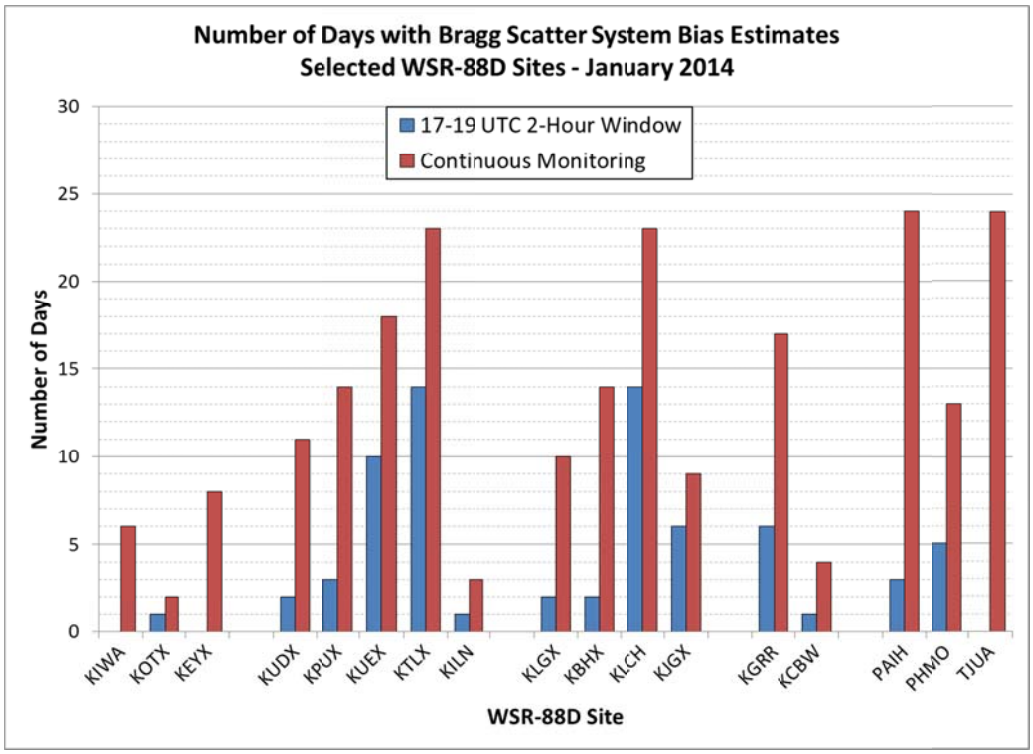

Figure 19. Same as Figure 18 but for January 2014.

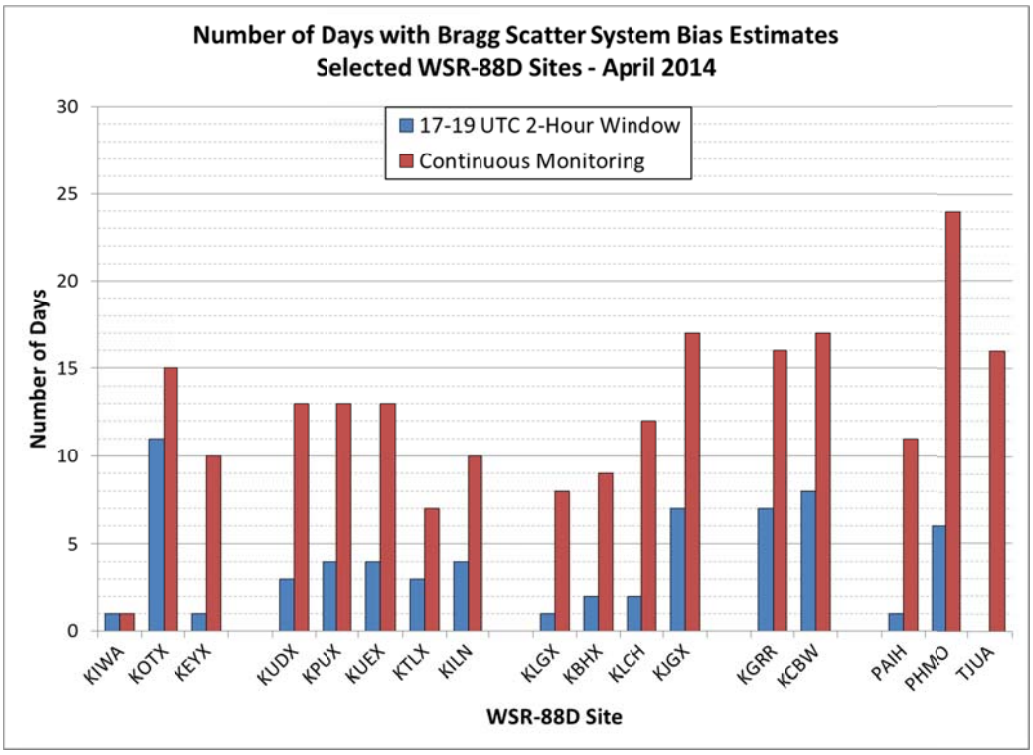

Figure 20. Same as Figure 18 but for April 2014.

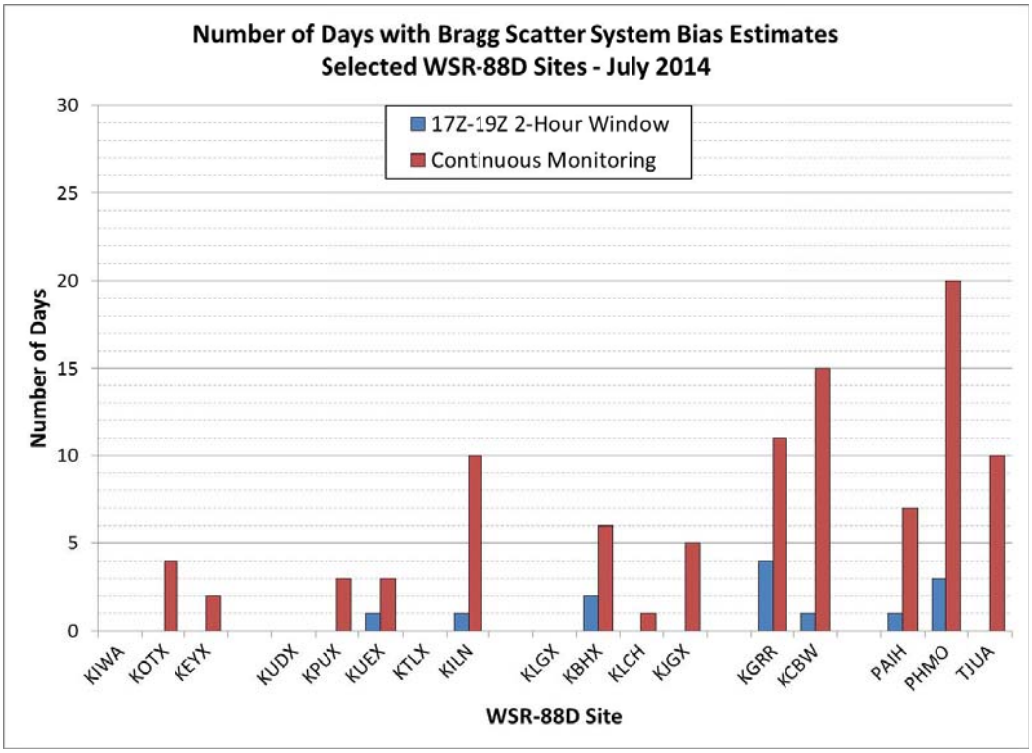

Figure 21. Same as Figure 18 but for July 2014.

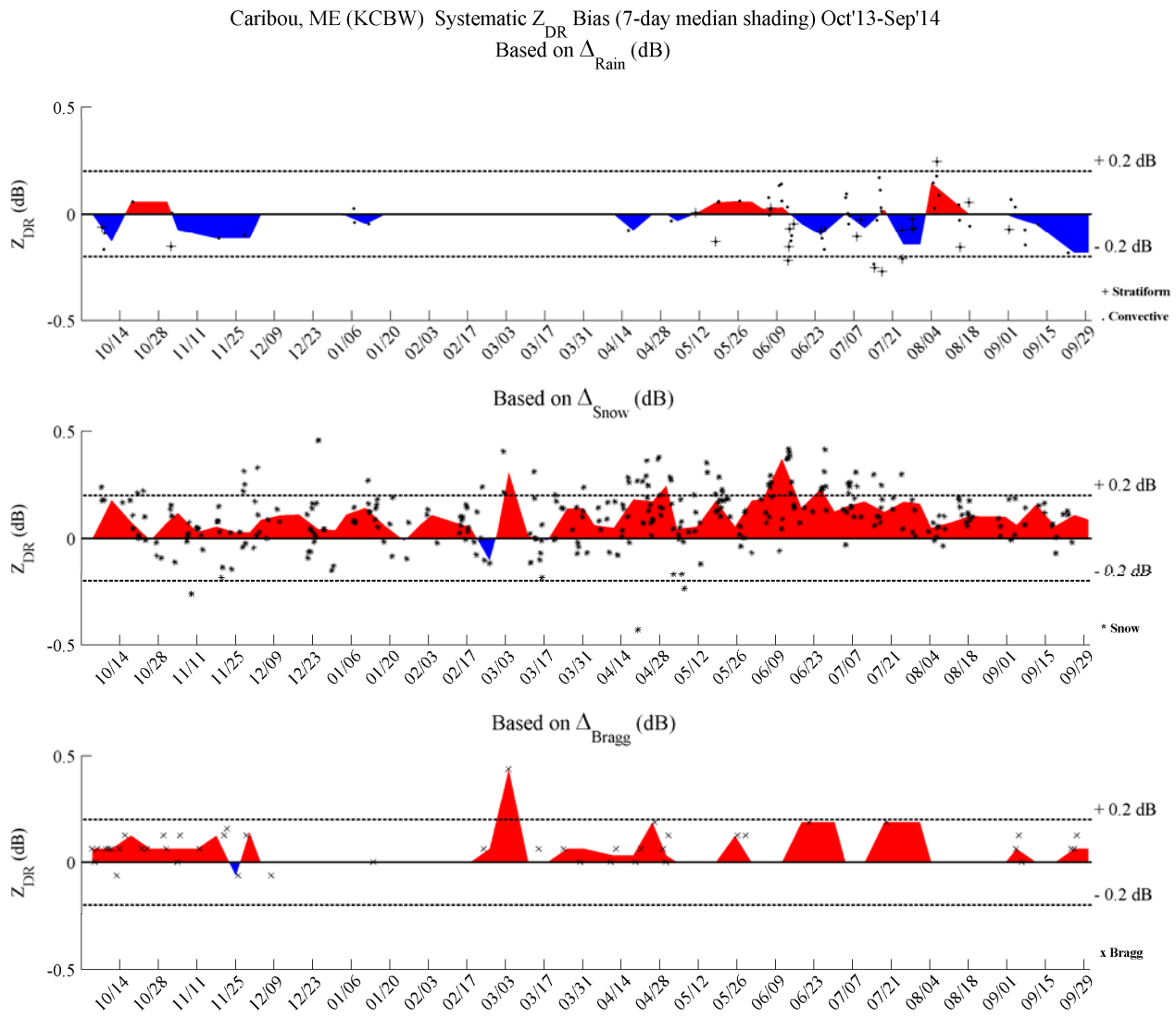

Figure 22. Shade chart for 1 October 2013 to 30 September 2014 for Caribou, ME (KCBW) comparing system Z_{DR} biases estimated from light rain (top panel), dry snow (middle panel), and Bragg scatter (bottom panel). Weekly medians for each method are used to fill in red shading for high biases and blue shading for low estimates. Individual estimates for light rain are shown as + or ·, for dry snow as ∗, and for Bragg scatter as x. For these methods, biases within ± 0.2 dB of 0 are generally considered acceptable.

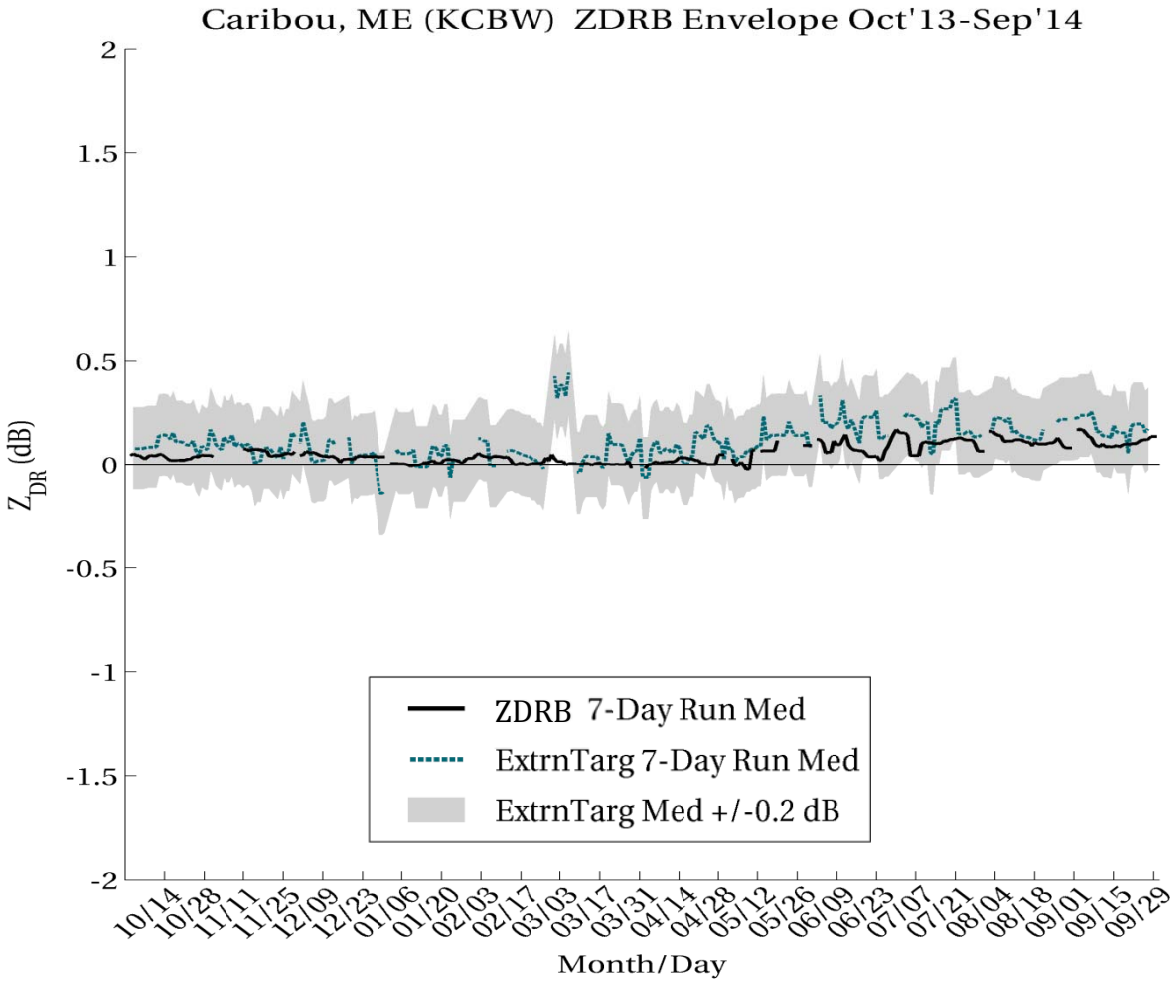

Figure 23. Chart comparing the engineering-estimated system Z_{DR} bias (solid black line) to the weather-estimated system Z_{DR} bias (dashed green line) for Caribou, ME for 1 October 2013 to 30 September 2014. The gray shading indicates a value ± 0.2 dB of the weather-based bias. Note the anomalously high values for the weather in early March also seen in Figure 22.